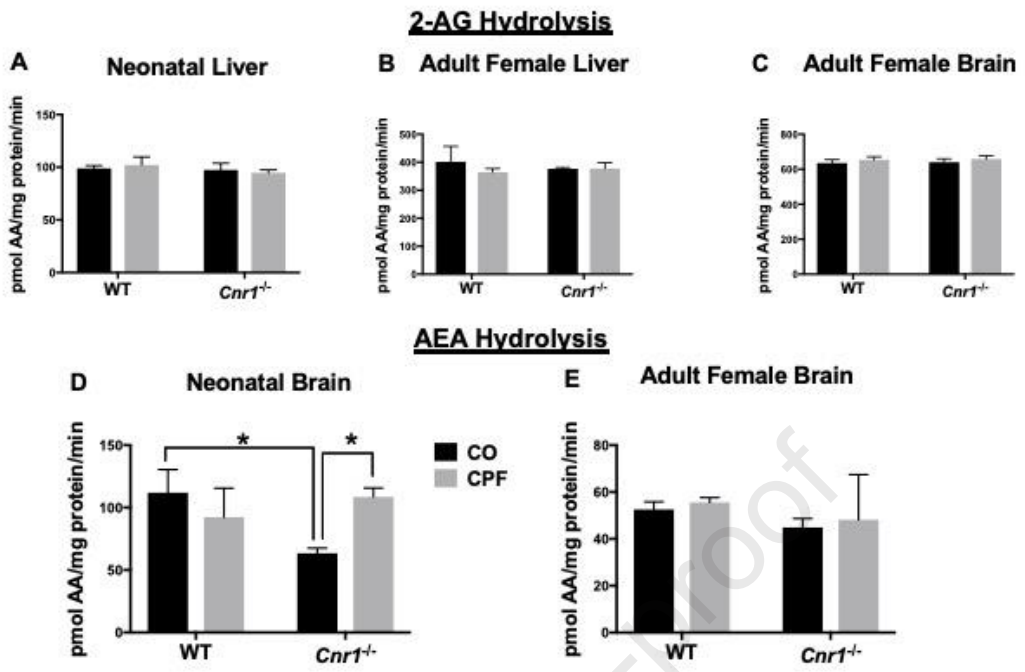

Supplemental Figure 1. 2-AG and AEA hydrolysis activity of tissue homogenates. 2-AG hydrolysis activities in whole-tissue homogenates of liver (A, B) and brain (C) from WT and *Cnr1*$^{-/-}$ adult female and/or mixed-sex neonatal mice. AEA hydrolysis activities in whole-tissue homogenates of brain (D, E) from WT and *Cnr1*$^{-/-}$ mice. Data are expressed as mean ± SD (n=3-5 mice per condition). *p<0.05 for indicated comparison.

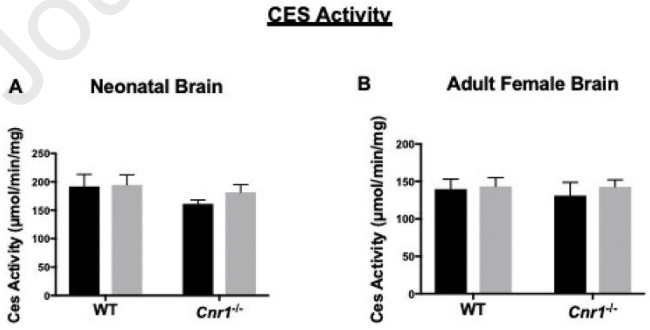

Supplemental Figure 2. Ces activity of tissue homogenates. Whole-tissue homogenates of brain from mixed-sex neonatal (A) and adult female (B) WT and *Cnr1*$^{-/-}$ mice. Data are presented as mean ± SD (n=3-5 mice per condition). None were

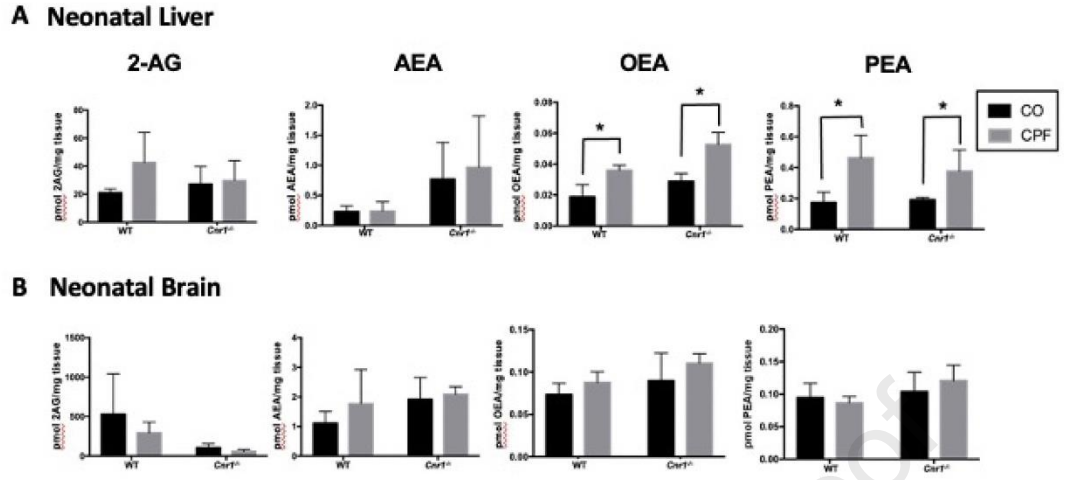

Supplemental Figure 3. eCB levels as measured by LC-MS/MS. A portion of the liver(A) and brain (B) from mixed-sex neonatal WT and *Cnr1*$^{-/-}$ mice was extracted for eCBs and quantified using deuterated standards (n=3-5). The resulting values were standardized by tissue weight. Data are expressed as mean ± SD, *p<0.05 for indicated comparison.

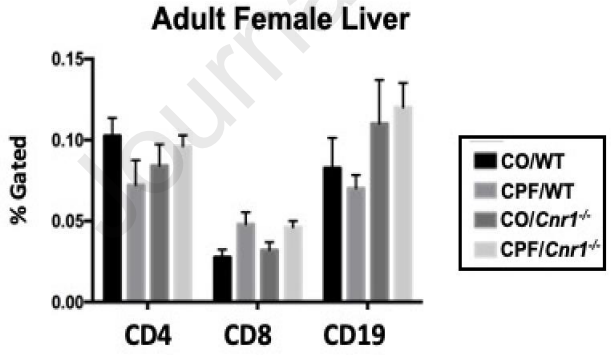

Supplemental Figure 4. Adaptive immune cell phenotypes by flow cytometry. Cells from WT and *Cnr1*$^{-/-}$ adult female livers (n=3-5) were stained for extracellular markers to identify T helper cells (CD4), cytotoxic T cells (CD8), and B cells (CD19). Data are expressed as the mean of percent lymphocyte gated ± SD. None were significant within cell surface marker group.

630 **Supplemental Table 1**. P values provided for treatment x genotype interactions.

631

632

633

634